

Covalent Au–C Contact Formation and C–C Homocoupling Reaction from Organotin Compounds in Single-Molecule Junctions

Weiyi Guo,[§] Yuhao Wu,[§] Chaochao Xie, Xuefeng Tan, Zhenpin Lu,* and Haixing Li*



Cite This: <https://doi.org/10.1021/jacs.4c03925>



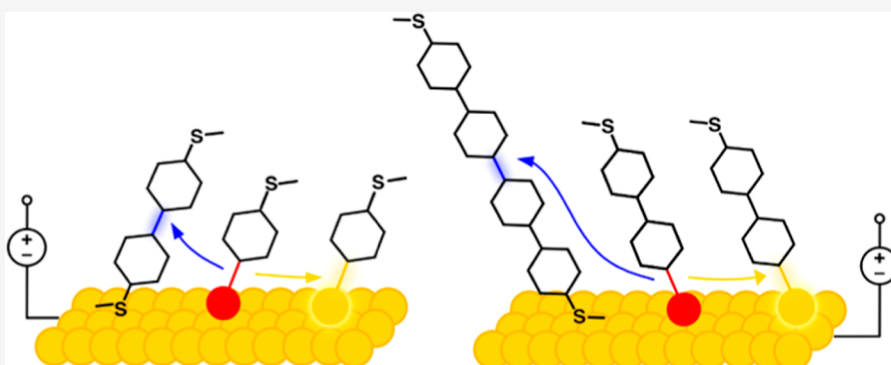
Read Online

ACCESS |

Metrics & More

Article Recommendations

Supporting Information



ABSTRACT: Formation of new chemical species has been achieved under an electric field by the use of the scanning tunneling microscope break junction technique, yet simultaneous implementation of catalytic reactions both at the organic/metal interface and in the bulk solution remains a challenging task. Herein, we show that *n*-butyl-substituted organotin-terminated benzene undergoes both an efficient cleavage of the terminal tributyltin group to form a covalent Au–C bond and a homocoupling reaction to yield biphenyl product when subjected to an electric field in the vicinity to Au electrodes. By using *ex situ* characterization of high-performance liquid chromatography with an UV–vis detector, we demonstrate that the homocoupling reaction can occur with high efficiency under an extremely low tip bias voltage of ~ 5 mV. Additionally, we show that the efficiency of the homocoupling reaction varies significantly in different solvents; the choice of the solvent proves to be one of the methods for modulating this reaction. By synthesizing and testing varied molecular backbone structures, we show that an extended biphenyl backbone undergoes homocoupling to form a quarterphenylene backbone, and the C–C coupling reactions are prohibited when additional aurophilic or bulky chemical groups that exhibit a steric blockage are introduced.

INTRODUCTION

When an organic chemical group is in contact with a metal surface to form molecular junctions, chemical reactions can occur not only between the organic compound and the metal but also among organic species. In addition to the donor–acceptor interaction, a robust covalent linkage between the molecule and the metal electrode can be achieved through chemical reactions in the terminal group. For example, Cheng et al., for the first time, reported that a direct Au–C contact is achieved *in situ* using trimethyl tin (SnMe_3)-terminated alkanes in scanning tunneling microscope break junction (STM-BJ) measurements (Scheme 1a).^{1,2} Similarly, cleavage of terminal groups such as iodide,³ boronic acid,⁴ diazonium group,⁵ trimethylsilyl group (in the presence of base),⁶ and hydrogen on acetylenes,^{7,8} as well as cleavage of the C–C bond in cycloparaphenylenes,⁹ have all been used to create covalent Au–C bonds at the molecule/Au interface.

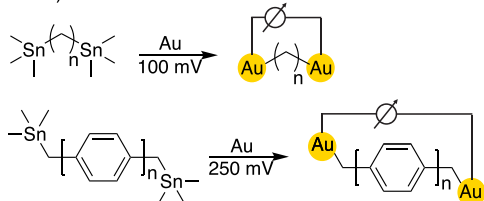
Moreover, the cleavage of terminal groups in the presence of Au electrodes can initiate further chemical reactions that lead to the formation of new species. For example, aryl iodides were

shown to undergo a Ullmann-type reaction to form an aryl–aryl bond in the presence of a polar solvent and a rough Au surface¹⁰ or with a nickel complex as the catalyst (Scheme 1b).¹¹ Compounds that are terminated with an amine group on one end and an L (L = thiol, thiomethyl, acetylene, or pyridine) group on the other have been demonstrated to undergo homocoupling reactions to form azobenzenes.¹² Additionally, a variety of chemical reactions, including homolysis,^{13,14} Diels–Alder,^{15–17} isomerization,¹⁸ etc., as well as the ones that are induced by an additional external control, such as light,^{19–24} a change in pH,^{22,25–27} and electrochemical gating^{28,29} have also been observed and characterized at the

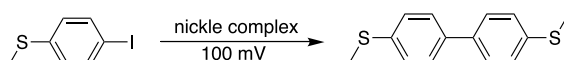
Received: March 20, 2024

Revised: September 12, 2024

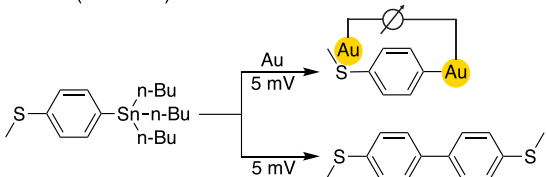
Accepted: September 13, 2024

Scheme 1. In situ Au–C and/or C–C Bond Formations in Single-Molecule Junctions under an Electric Fielda In situ $-\text{Sn}(\text{Me})_3$ cleavage (Hybertsen, Breslow, and Venkataraman, 2011)

b In situ aryl iodide homocoupling reaction (Steigerwald, Nuckolls, and Venkataraman, 2022)



c In situ n-butyl-substituted organotin cleavage and homocoupling reaction (this work)

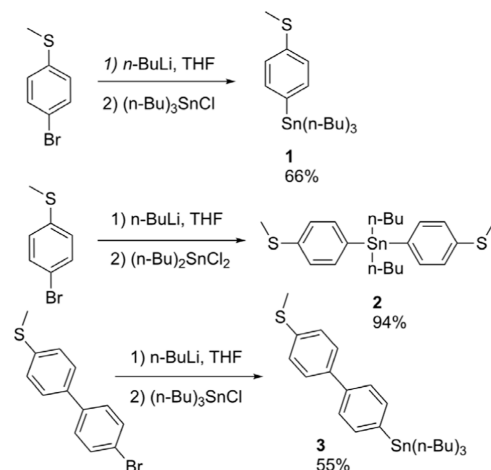


single-molecule level. It remains rare to observe both an efficient cleavage of the terminal group for forming Au–C covalent bond and effective chemical reactions for generating new organic products simultaneously in one system, and even if both occur, either the prior dominates the reactions,² or a high bias voltage is needed for promoting the latter.⁴

In the present work, we show that with an electric field and Au electrodes, *n*-butyl-substituted organotin-terminated ($-\text{Sn}(n\text{-Bu})_3$) benzenes cleave to form a covalent Au–C bond at the molecule/electrode contact and undergo a C–C coupling reaction to generate biphenyls (Scheme 1c). Notably, our approach for both a Au–C linkage and homocoupling reaction in one system requires a low bias voltage of ~ 5 mV. The in situ formation of two species that contain either a Au–C or a C–C bond is evidenced by the observation of two distinct single-molecule junction conductance signatures, i.e., the conductance values and junction elongation lengths. We confirm the formation of a biphenyl, a C–C homocoupling product, by comparing the single-molecule junction conductance data of the $-\text{Sn}(n\text{-Bu})_3$ -terminated monomer with that of the ex situ synthesized biphenyl compound and analyzing the STM-BJ reaction products with high-performance liquid chromatography (HPLC). We further find that Au–C formation occurs in all solvents that we test, while the homocoupling reaction occurs only in selective solvents. Moreover, our results show that this approach for catalyzing homocoupling reactions can be applied to a longer biphenyl backbone for in situ forming the quarterphenylene as well.

RESULTS AND DISCUSSION

Synthesis. The synthesis of organotin compound tributyl(4-(methylthio)phenyl)stannane (**1**), dibutylbis(4-(methylthio)phenyl)stannane (**2**), and tributyl(4'-(methylthio)-[1',1'-biphenyl]-4-yl)stannane (**3**) was realized through transmetalation with organolithium species and organotin halides (Scheme 2; details are given in the Supporting Information Section I). All three compounds (**1**–**3**) appeared

Scheme 2. Synthesis of Compounds **1, **2**, and **3****

as oil liquids. Compound **1** was purified by a fractional distillation. Both compounds **2** and **3** were purified via column chromatography. All of the compounds (**1**–**3**) were fully characterized by NMR spectra and high-resolution mass spectrometry (Supporting Information Sections I and IV).

Analysis of In Situ Reactions in STM-BJ Experiments.

We first perform the single-molecule conductance measurements of a solution of 1 mM **1** (chemical structure in Figure 1a) in 1,2,4-trichlorobenzene (TCB) solvent at a 5 mV tip bias using the STM-BJ method (details are given in the Supporting Information Section II).^{30–32} We observe individual conductance traces that exhibit a molecular conductance plateau at a high conductance, at a low conductance, or containing a high-to-low transition, as displayed in Figure 1b. We collect conductance traces over 6 h and generate logarithmically binned one-dimensional (1D) and two-dimensional (2D) histograms over the time course without data selection. As shown in Figure 1c,d, we observe a conductance peak at $6.8 \times 10^{-3} G_0$ ($G_0 = 2e^2/h$) with a molecular elongation length of ~ 0.17 nm from the measurement in the first hour, which we ascribe to the cleavage of the $-\text{Sn}(n\text{-Bu})_3$ group and formation of **A1** junction (Figure 1a) as the conductance value and junction elongation length agree with the previously reported data.^{3,4,33}

In stark contrast, a clear conductance signature at $1.0 \times 10^{-3} G_0$ with an elongation length of 0.39 nm appears from conductance measurements during 1–3 h (Figure 1e,f). We propose that this low conductance peak arises from the formation of biphenyl **P2** (chemical structure in Figure 1a), a C–C coupling product. As the measurement proceeds, this low conductance plateau is continuously observed, as shown in Figure S1. To test our hypothesis, we further carry out conductance experiments of ex situ synthesized **P2** under a 90 mV bias voltage and observe a conductance peak at $1.4 \times 10^{-3} G_0$ with a molecular elongation length of 0.41 nm (Figure 1g,h), agreeing well with what was observed for the 3 h measurement of **1**. We additionally test the voltage-dependence of both Au–C formation and homocoupling reaction by comparing the conductance measurements of **1** under 5, 225, 450, and 900 mV tip bias voltages over the course of 6 h (Figures 1 and S1–S4). If we assume that the impact of the applied bias voltage on the junction formation probability is minimal,³⁴ then based on the observed peak intensity change with measured time, we conclude a similar Au–C formation

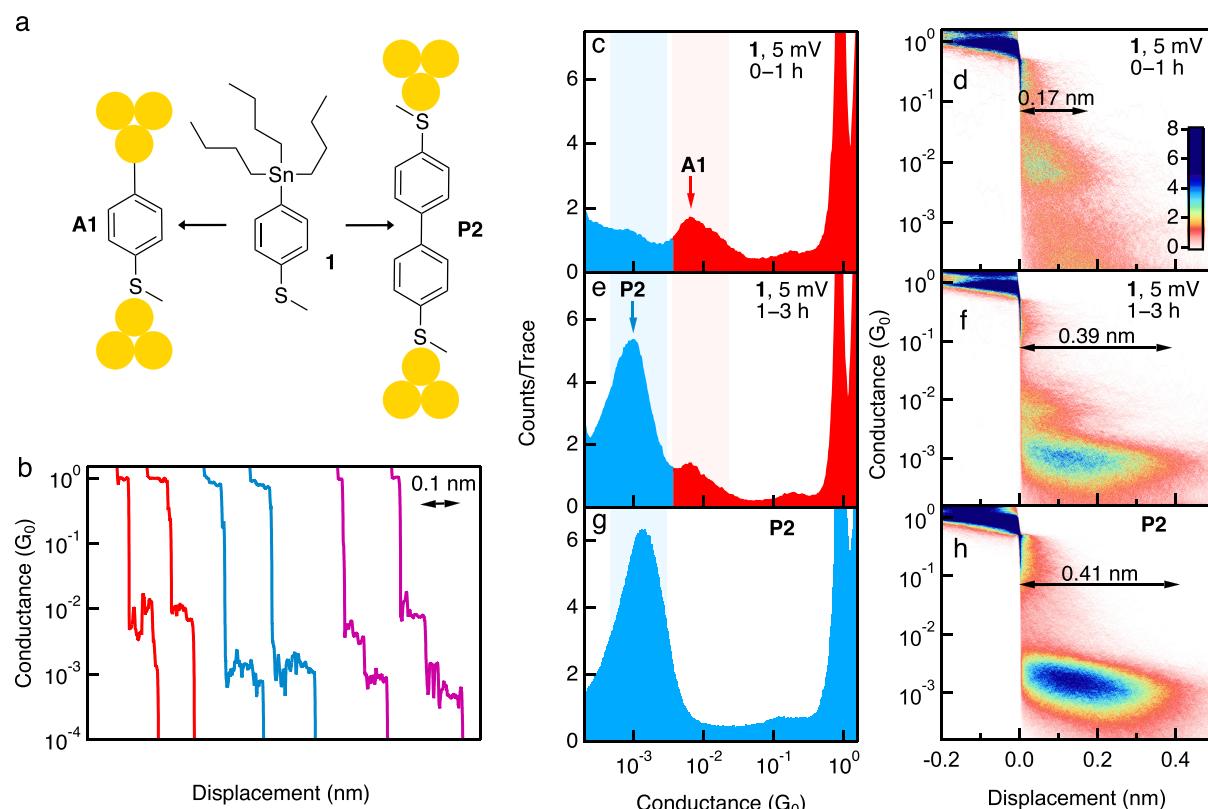


Figure 1. (a) Schematic illustration of chemical reactions of **1** that occur in STM-BJ experiments. (b) Representative individual traces showing the ~ 0.17 nm high conductance plateau (red), ~ 0.39 nm low conductance plateau (blue), and high-to-low transition plateau (purple) observed for **1** measured in TCB. (c) Logarithmically binned 1D and (d) 2D histograms of **1** measured in TCB under a 5 mV tip bias from 0–1 h. (e) 1D and (f) 2D histograms of **1** measured under the same condition as in (c,d) in 1–3 h. (g) 1D and (h) 2D histograms of ex situ synthesized **P2** measured in TCB under a 90 mV tip bias. Arrows in (d,f,h) indicate the molecular junction elongation length determined from 2D histograms. We create 1D line profiles along the displacement axis by integrating all counts in the 2D conductance histograms and obtain the junction elongation length by locating where the line profile drops to 20% of its peak intensity.

reaction efficiency and a decreasing homocoupling reaction efficiency with increasing applied bias voltages in the 5–900 mV bias voltage range. We note that our measurements of ex situ synthesized **P2** under 5 mV (Figure S5) and 90 mV (Figure 1g) suggest that higher applied voltage can possibly decrease the molecular junction formation probability, therefore believe that this effect can also contribute to a decreased **P2** conductance peak intensity under increasing bias voltages, as seen in our in situ reaction experiments of **1**.

Over the course of the measurement during 3–12 h of **1** under 225 mV, 39,000 conductance traces are collected. We expect four scenarios of the molecular conductance plateaus in these individual traces: a high conductance state only, a low conductance state only, both high and low conductance states, and no conductance feature. We then perform a trace-by-trace analysis to categorize the traces into these four groups. We find that $\sim 31\%$ of the traces are high-state-only (example in Figure 1b, red), $\sim 42\%$ are high-to-low (example in Figure 1b, purple), $<1\%$ are low-state-only (example in Figure 1b, blue), and the rest 27% of the traces show no clear molecular plateau features (high state $\sim 6.8 \times 10^{-3} G_0$, low state $\sim 1.0 \times 10^{-3} G_0$, histograms of the grouped traces are seen in Figure S6). This indicates that an **A1** to **P2** transition during one junction formation is not a rare event, suggesting that the C–C homocoupling reaction likely occurs immediately after two $-\text{Sn}(n\text{-Bu})_3$ groups cleave in proximity. We indeed observe a broad conductance peak with a tail on the higher conductance

side in measurement of **1** in TCB (Figure 1c); by categorization of the traces into two groups (Figure S7), we see a $\sim 6.8 \times 10^{-3} G_0$ conductance peak for **A1** junction and a second peak at $\sim 1.2 \times 10^{-2} G_0$. In the measurement of **1** in tetradecane (TD), we observe two peaks at similar conductance values (Figure S8). We speculate that this $\sim 1.2 \times 10^{-2} G_0$ conductance state, around 2 times of the **A1** junction conductance, possibly arises from junctions of two molecules attached between the tip and the substrate in parallel.^{35–38} The probability for capturing two molecules in parallel between the Au electrodes immediately after the rupture of the Au–Au contact is considerably low, but nonetheless, the presence of two-molecule parallel-bridged junctions suggests that two or more $-\text{Sn}(n\text{-Bu})_3$ groups cleave in proximity in the process of forming and breaking junctions.

Next, we carry out STM-BJ measurements of **1** in tetradecane (TD), 1,3,5-trimethylbenzene (TMB), and 2-methoxyethyl ether (2-ME) to investigate the effect of the solvent on the observed Au–C formation and homocoupling reaction. We find that only the transmetalation reaction, but not the homocoupling reaction, occurs in TD (Figure S8) and TMB (Figure S9), and both reactions occur in 2-ME (Figure S10). We refer to the literature which suggests that in bulk solution reactions, solvent with high dielectric constant promotes homocoupling reactions^{39–41} and conclude that our results for the most part align with this general understanding (dielectric constant is ~ 2.03 for TD, 2.24 for

TCB, 2.4 for TMD, and 7.3 for 2-ME).⁴² We note that further investigation is needed to elucidate the role of solvent in regulating the transmetalation and homocoupling reactions observed for **1**. Additionally, we compare the experiments performed with an atomically flat Au-coated mica substrate with results of using a rough Au-coated steel substrate. We do not observe a clear conductance peak for **P2** junctions for experiments performed with a flat substrate (Figure S11), in contrast to the well-defined signatures for **P2** junctions when a rough substrate was used (all experiments in this work except for Figure S11). We observe the conductance peak for **A1** junctions with similar intensity from experiments performed with either a flat or a rough Au substrate. We thus propose that the uncoordinated Au atoms present in rough Au surfaces can act as active catalytic sites for homocoupling reactions, in agreement with a previous report.¹⁰

As a further confirmation of the formation of **P2**, we next analyze the solutions from STM-BJ measurements of **1** using HPLC. We find that after 1 mM **1** was under STM-BJ measurement with a 5 mV tip bias voltage for 3 h, a new peak in HPLC spectrum at the same location as the one for ex situ synthesized **P2** appears, indicating the detection of in situ formed **P2** in STM-BJ measurements of **1** (Figure 2, with the

C–C coupling reaction does not happen exclusively in the metal–molecule–metal junction. We also observe an appearance of a second new peak at \sim 3.5 min for the measurement of the STM-BJ solution (Figure 2b) and confirm that this peak arises from the TCB solvent that we have used in single-molecule conductance measurements. As for the resulting *n*-butyl-substituted tin fragments from the cleavage reaction, they are likely bound on the Au surface through Au–Sn bonds, as shown previously.^{2,43}

We next evaluate whether the applied electric field is a required condition for the organotin cleavage and homocoupling reactions. Previous reports of STM-BJ and X-ray photoemission spectroscopy measurements^{2,43} have shown that the trimethyltin cleavage reaction occurs once the $\text{Sn}(\text{Me})_3$ -terminated compound is deposited on the Au metal surface in the absence of an applied external electric field. Here, we perform HPLC analysis of a solution of **1** that was placed on an Au substrate for 3 h and observe no formation of **P2** as no peak is seen at around 6 min retention time (Figure S16). This result suggests that an applied electric field is required for the homocoupling reaction.

We next investigate whether the cleavage and homocoupling reaction can occur when the *n*-butyl-substituted tin group is part of the molecular backbone using the molecule **2** (chemical structure is shown in Figure 3a). We conduct the single-molecule conductance measurements of 1 mM **2** in TCB under 900 mV for 6 h. We observe a clear conductance peak located at around $6.8 \times 10^{-3} G_0$ (Figure 3b) with a molecular junction elongation length of 0.19 nm (Figure 3c), consistent with the high conductance state observed for **1**. These results demonstrate that the organotin group was cleaved, leading to the formation of a Au–C covalent contact and **A1** junction. Besides, a new conductance peak at $1.6 \times 10^{-5} G_0$ with a molecular elongation length of 0.52 nm is observed in the measurement of **2** (Figure 3b,c). We suggest that this ultralow conductance peak corresponds to the molecular junctions formed by **2** itself.

The lack of clear conductance signature at $1.0 \times 10^{-3} G_0$ in both 1D and 2D histograms indicates that either the homocoupling reaction does not occur with a detectable efficiency, or the biphenyl is formed, but **A1** and **2** outcompete the biphenyl **P2** in forming molecular junctions during the measurement. To distinguish these two possibilities, we analyze the STM-BJ measurement solution using HPLC and do not observe a peak for **P2** (Figure S17), indicating a very low efficiency for the homocoupling reactions in the STM-BJ measurement of **2**. We hypothesize that the steric hindrance of the phenyl ring as well as the presence of a second aurophilic thiomethyl group in **2** prohibit dual transmetalation reactions from occurring in proximity, resulting in a significantly lowered chance for homocoupling reactions. We additionally study the voltage-dependence for the cleavage and possible homocoupling reaction of **2** and observe the same $\sim 6.8 \times 10^{-3} G_0$ conductance state and no clear peak at $1.0 \times 10^{-3} G_0$ under tip bias voltages of 5 mV (Figure S18), 225 mV (Figure S19), and 900 mV, suggesting similar efficiency of the Au–C formation and absence of homocoupling reaction under all tested bias voltages between 5 and 900 mV. This observation, similar to the results of **1**, confirms the proposition that an electric field is not required for Au–C formation. A summary of possible single-molecule junctions formed in an STM-BJ measurement of **2** is shown in Figure 3a.

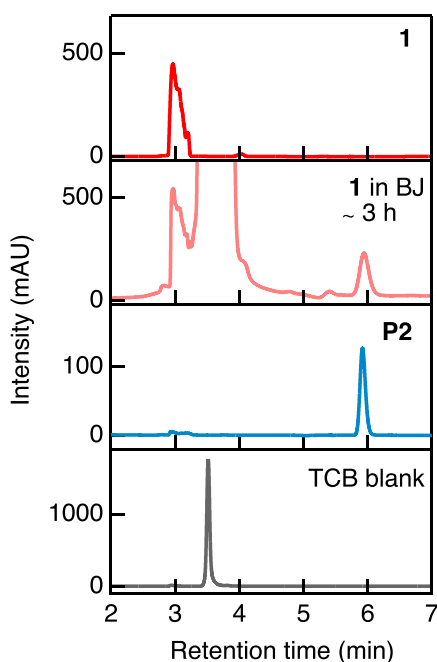


Figure 2. HPLC results of (a) **1**, (b) **1** in TCB subject to STM-BJ measurements for 3 h under 5 mV, (c) ex situ synthesized **P2**, and (d) TCB blank. The intensity in (b) is multiplied by 20 so that the spectra in (a,b) have similar peak height at 3 min retention time.

corresponding conductance histograms of the STM-BJ measurement and a comparison of the HPLC spectra of **1** in different mobile phases shown in Figures S12 and S13). As shown in Figure 2b, the relative intensity of the new peak at \sim 6 min retention time in comparison to the peak of **1** at \sim 3 min suggests a high efficiency of the homocoupling reaction. By comparing the integrated area for the peak corresponding to **P2** in the HPLC spectrum for the STM-BJ solution and that for a pure 0.3 mM **P2** solution, we approximate that a starting 50 nmol **1** yields about 13 nmol **P2** in this experiment (details are given in Figures S14 and S15). This result indicates that the

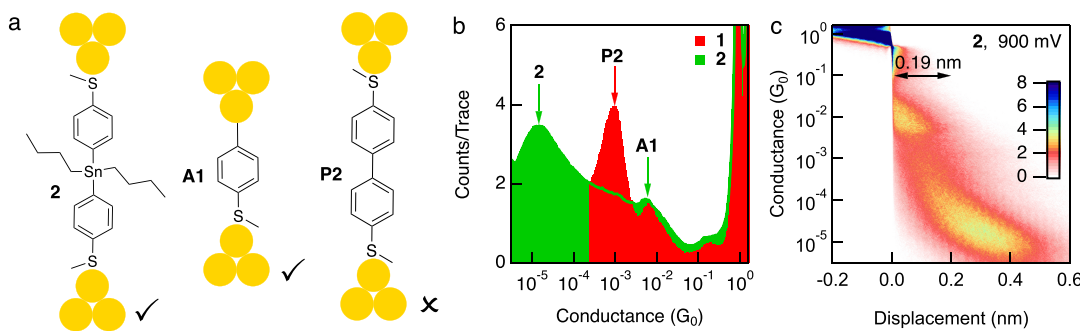


Figure 3. (a) Schematic illustration of possible molecular junctions formed in STM-BJ experiments of **2**. (b) Logarithmically binned 1D histograms of **1** and **2** measured in TCB under 5 and 900 mV, respectively. (c) 2D histogram of **2** created from the same data that were used to generate the 1D histogram in (b).

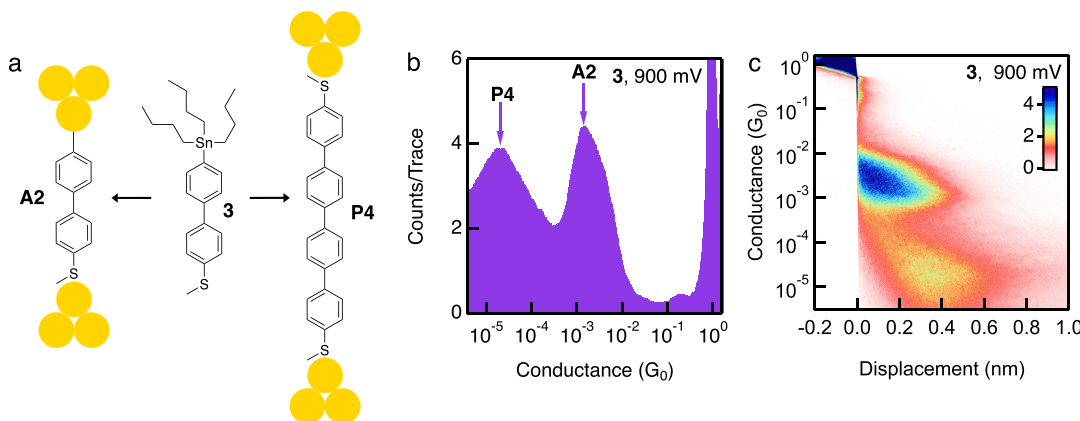


Figure 4. (a) Schematic illustration of chemical reactions of **3** that occur in STM-BJ experiments. (b) 1D and (c) 2D conductance histograms of 0.1 mM **3** in TCB measured under 900 mV. To display the intensity of both conductance features, the color scale is adjusted as denoted in the color bar.

We next test whether the *in situ* reactions of **1** are specific to the molecular backbone benzene, therefore we measure the *n*-butyl-substituted organotin-terminated biphenyl derivative **3** (chemical structure is given in Figure 4a) in STM-BJ. In detail, we subject a 0.1 mM solution of **3** in TCB under a 900 mV tip bias in break junction measurements for 6 h. We observe two clear conductance peaks located at $\sim 1.5 \times 10^{-3} G_0$ and $2.0 \times 10^{-5} G_0$, respectively, in the 1D histogram (Figure 4b). The molecular elongation length corresponding to the high and low conductance peaks are 0.40 and 0.84 nm, as shown in Figure 4c. We assign the high conductance state to junctions of **A2** as a result of the organotin group cleavage and assign the low conductance signature to junctions of **P4** formed from the C–C bond homocoupling reactions (illustration of the junctions is given in Figure 4a). The observed conductance peak values and junction elongation lengths of the two peaks of **3** are in good agreement with the previously reported data of the same **A2** and **P4** molecular junctions.^{3,4,33}

We additionally perform the single-molecule conductance measurement of **3** under a -900 mV tip bias and observe the same conductance signatures monitored during a 6 h measurement as those seen in the measurement of **3** under 900 mV (Figures S20 and S21). Comparing the measurement results of **3** under 900 and -900 mV, we conclude that the polarity of the tip bias potential does not affect the efficiency of the reactions. Similar to the conductance peak of **A1**, **A2** conductance peak shows an asymmetric distribution with a broader tail on the high conductance side, which is indicative of possible junction formations with two molecules bridging in

between the two Au electrodes in parallel³⁵ (analysis is given in Figure S22) and suggests the availability of two or more cleaved species in proximity for next-step homocoupling reactions. This result demonstrates the general application of this approach in achieving an efficient transmetalation and homocoupling reaction with varied molecular backbone designs.

CONCLUSIONS

In summary, we have synthesized a series of $-\text{Sn}(n\text{-Bu})_3$ -substituted polyphenyl-chain molecules and demonstrated that the formation of covalent Au–C and C–C bonds can be achieved by an STM-BJ technique. The formation of the C–C coupling product is monitored by conductance measurements *in situ* at the single-molecule level and confirmed *ex situ* by HPLC analysis. Importantly, an applied bias voltage as low as ~ 5 mV can efficiently catalyze the C–C homocoupling. We find that the efficiency of the homocoupling reaction can be regulated by the use of solvent as well as the chemical structure of the molecular backbone. Taken together, we envisage that this method of creating covalent Au–C and C–C linkages will be further expanded for use in activating chemical bonds and synthesizing molecules at organic–metal interfaces by an electric field, offering a toolbox for reaction manipulation.

ASSOCIATED CONTENT

Supporting Information

The Supporting Information is available free of charge at <https://pubs.acs.org/doi/10.1021/jacs.4c03925>.

Synthetic procedures, experimental procedures, additional information, and characterization data ([PDF](#))

AUTHOR INFORMATION

Corresponding Authors

Zhenpin Lu — Department of Chemistry, City University of Hong Kong, Kowloon 999077 Hong Kong SAR, China;
 orcid.org/0000-0003-0000-6026; Email: zhenpilu@cityu.edu.hk

Haixing Li — Department of Physics, City University of Hong Kong, Kowloon 999077 Hong Kong SAR, China;
 orcid.org/0000-0002-1383-4907; Email: haixinli@cityu.edu.hk

Authors

Weiyi Guo — Department of Physics, City University of Hong Kong, Kowloon 999077 Hong Kong SAR, China;
 orcid.org/0000-0001-6350-8950

Yuhao Wu — Department of Chemistry, City University of Hong Kong, Kowloon 999077 Hong Kong SAR, China

Chaochao Xie — Department of Chemistry, City University of Hong Kong, Kowloon 999077 Hong Kong SAR, China

Xuefeng Tan — Department of Chemistry, City University of Hong Kong, Kowloon 999077 Hong Kong SAR, China

Complete contact information is available at:

<https://pubs.acs.org/10.1021/jacs.4c03925>

Author Contributions

W.G. and Y.W. contributed equally to this work.

Notes

The authors declare no competing financial interest.

ACKNOWLEDGMENTS

This work is primarily funded by a Strategic Interdisciplinary Research Grant (7020095) from the City University of Hong Kong. Single-molecule charge transport experimental work is partly supported by the Research Grants Council of the Hong Kong SAR, China (project nos. 21310722 and 11304723) and the City University of Hong Kong through a start-up fund (9610521). Synthetic work is partly supported by the Research Grants Council of the Hong Kong SAR, China (project no. 11306523).

REFERENCES

- Chen, W.; Widawsky, J. R.; Vázquez, H.; Schneebeli, S. T.; Hybertsen, M. S.; Breslow, R.; Venkataraman, L. Highly conducting π -conjugated molecular junctions covalently bonded to gold electrodes. *J. Am. Chem. Soc.* **2011**, *133* (43), 17160–17163.
- Cheng, Z.-L.; Skouta, R.; Vazquez, H.; Widawsky, J. R.; Schneebeli, S.; Chen, W.; Hybertsen, M. S.; Breslow, R.; Venkataraman, L. In situ formation of highly conducting covalent Au–C contacts for single-molecule junctions. *Nat. Nanotechnol.* **2011**, *6* (6), 353–357.
- Starr, R. L.; Fu, T.; Doud, E. A.; Stone, I.; Roy, X.; Venkataraman, L. Gold–carbon contacts from oxidative addition of aryl iodides. *J. Am. Chem. Soc.* **2020**, *142* (15), 7128–7133.
- Li, Y.; Zhao, C.; Wang, R.; Tang, A.; Hong, W.; Qu, D.; Tian, H.; Li, H. In Situ Monitoring of Transmetallation in Electric Potential-Promoted Oxidative Coupling in a Single-Molecule Junction. *CCS Chem.* **2023**, *5* (1), 191–199.
- Hines, T.; Díez-Pérez, I.; Nakamura, H.; Shimazaki, T.; Asai, Y.; Tao, N. Controlling formation of single-molecule junctions by electrochemical reduction of diazonium terminal groups. *J. Am. Chem. Soc.* **2013**, *135* (9), 3319–3322.
- Hong, W.; Li, H.; Liu, S.-X.; Fu, Y.; Li, J.; Kaliginedi, V.; Decurtins, S.; Wandlowski, T. Trimethylsilyl-terminated oligo(phenylene ethynylene)s: an approach to single-molecule junctions with covalent Au–C σ -bonds. *J. Am. Chem. Soc.* **2012**, *134* (47), 19425–19431.
- Bejarano, F.; Olavarria-Contreras, I. J.; Droghetti, A.; Rungger, I.; Rudnev, A.; Gutiérrez, D.; Mas-Torrent, M.; Veciana, J.; Van Der Zant, H. S.; Rovira, C.; Burzurí, E.; Civillers, N. Robust organic radical molecular junctions using acetylene terminated groups for C–Au bond formation. *J. Am. Chem. Soc.* **2018**, *140* (5), 1691–1696.
- Olavarria-Contreras, I. J.; Perrin, M. L.; Chen, Z.; Klyatskaya, S.; Ruben, M.; van der Zant, H. S. J. C–Au Covalently Bonded Molecular Junctions Using Nonprotected Alkynyl Anchoring Groups. *J. Am. Chem. Soc.* **2016**, *138* (27), 8465–8469.
- Lin, J.; Lv, Y.; Song, K.; Song, X.; Zang, H.; Du, P.; Zang, Y.; Zhu, D. Cleavage of non-polar C(sp²)–C(sp²) bonds in cycloparaphenylenes via electric field-catalyzed electrophilic aromatic substitution. *Nat. Commun.* **2023**, *14* (1), 293.
- Stone, I. B.; Starr, R. L.; Hoffmann, N.; Wang, X.; Evans, A. M.; Nuckolls, C.; Lambert, T. H.; Steigerwald, M. L.; Berkelbach, T. C.; Roy, X.; Venkataraman, L. Interfacial electric fields catalyze Ullmann coupling reactions on gold surfaces. *Chem. Sci.* **2022**, *13* (36), 10798–10805.
- Orchianian, N. M.; Guizzo, S.; Steigerwald, M. L.; Nuckolls, C.; Venkataraman, L. Electric-field-induced coupling of aryl iodides with a nickel (0) complex. *Chem. Commun.* **2022**, *58* (90), 12556–12559.
- Zang, Y.; Stone, I.; Inkpen, M. S.; Ng, F.; Lambert, T. H.; Nuckolls, C.; Steigerwald, M. L.; Roy, X.; Venkataraman, L. In Situ Coupling of Single Molecules Driven by Gold-Catalyzed Electro-oxidation. *Angew. Chem., Int. Ed.* **2019**, *58* (45), 16008–16012.
- Zhang, B.; Schaack, C.; Prindle, C. R.; Vo, E. A.; Aziz, M.; Steigerwald, M. L.; Berkelbach, T. C.; Nuckolls, C.; Venkataraman, L. Electric fields drive bond homolysis. *Chem. Sci.* **2023**, *14* (7), 1769–1774.
- Li, H.; Kim, N. T.; Su, T. A.; Steigerwald, M. L.; Nuckolls, C.; Darancet, P.; Leighton, J. L.; Venkataraman, L. Mechanism for Si–Si bond rupture in single molecule junctions. *J. Am. Chem. Soc.* **2016**, *138* (49), 16159–16164.
- Aragones, A. C.; Haworth, N. L.; Darwish, N.; Ciampi, S.; Mannix, E. J.; Wallace, G. G.; Diez-Perez, I.; Coote, M. L. Electrostatic catalysis of a Diels–Alder reaction. *Nature* **2016**, *531* (7592), 88–91.
- Huang, X.; Tang, C.; Li, J.; Chen, L.-C.; Zheng, J.; Zhang, P.; Le, J.; Li, R.; Li, X.; Liu, J.; Yang, Y.; Shi, J.; Chen, Z.; Bai, M.; Zhang, H.-L.; Xia, H.; Cheng, J.; Tian, Z.-Q.; Hong, W. Electric field-induced selective catalysis of single-molecule reaction. *Sci. Adv.* **2019**, *5* (6), No. eaaw3072.
- Yang, C.; Liu, Z.; Li, Y.; Zhou, S.; Lu, C.; Guo, Y.; Ramirez, M.; Zhang, Q.; Li, Y.; Liu, Z.; Houk, K. N.; Zhang, D.; Guo, X. Electric field-catalyzed single-molecule Diels–Alder reaction dynamics. *Sci. Adv.* **2021**, *7* (4), No. eabf0689.
- Zang, Y.; Zou, Q.; Fu, T.; Ng, F.; Fowler, B.; Yang, J.; Li, H.; Steigerwald, M. L.; Nuckolls, C.; Venkataraman, L. Directing isomerization reactions of cumulenes with electric fields. *Nat. Commun.* **2019**, *10* (1), 4482.
- Meng, L.; Xin, N.; Hu, C.; Wang, J.; Gui, B.; Shi, J.; Wang, C.; Shen, C.; Zhang, G.; Guo, H.; Meng, S.; Guo, X. Side-group chemical gating via reversible optical and electric control in a single molecule transistor. *Nat. Commun.* **2019**, *10* (1), 1450.
- Kim, Y.; Garcia-Lekue, A.; Sysoiev, D.; Frederiksen, T.; Groth, U.; Scheer, E. Charge Transport in Azobenzene-Based Single-Molecule Junctions. *Phys. Rev. Lett.* **2012**, *109* (22), 226801.

- (21) Roldan, D.; Kaliginedi, V.; Cobo, S.; Kolivoska, V.; Bucher, C.; Hong, W.; Royal, G.; Wandlowski, T. Charge Transport in Photoswitchable Dimethyldihryptopyrene-Type Single-Molecule Junctions. *J. Am. Chem. Soc.* **2013**, *135* (16), 5974–5977.
- (22) Darwish, N.; Aragonès, A. C.; Darwish, T.; Ciampi, S.; Díez-Pérez, I. Multi-Responsive Photo- and Chemo-Electrical Single-Molecule Switches. *Nano Lett.* **2014**, *14* (12), 7064–7070.
- (23) Sendler, T.; Luka-Guth, K.; Wieser, M.; Lokamani; Wolf, J.; Helm, M.; Gemming, S.; Kerbusch, J.; Scheer, E.; Huhn, T.; Erbe, A. Light-Induced Switching of Tunable Single-Molecule Junctions. *Adv. Sci.* **2015**, *2* (5), 1500017.
- (24) Jia, C.; Migliore, A.; Xin, N.; Huang, S.; Wang, J.; Yang, Q.; Wang, S.; Chen, H.; Wang, D.; Feng, B.; Liu, Z.; Zhang, G.; Qu, D.-H.; Tian, H.; Ratner, M. A.; Xu, H. Q.; Nitzan, A.; Guo, X. Covalently bonded single-molecule junctions with stable and reversible photo-switched conductivity. *Science* **2016**, *352* (6292), 1443–1445.
- (25) Herrer, I. L.; Ismael, A. K.; Milán, D. C.; Vezzoli, A.; Martín, S.; González-Orive, A.; Grace, I.; Lambert, C.; Serrano, J. L.; Nichols, R. J.; Cea, P. Unconventional Single-Molecule Conductance Behavior for a New Heterocyclic Anchoring Group: Pyrazolyl. *J. Phys. Chem. Lett.* **2018**, *9* (18), 5364–5372.
- (26) Scullion, L.; Doneux, T.; Bouffier, L.; Fernig, D. G.; Higgins, S. J.; Bethell, D.; Nichols, R. J. Large Conductance Changes in Peptide Single Molecule Junctions Controlled by pH. *J. Phys. Chem. C* **2011**, *115* (16), 8361–8368.
- (27) Chen, F.; Li, X.; Hihath, J.; Huang, Z.; Tao, N. Effect of Anchoring Groups on Single-Molecule Conductance: Comparative Study of Thiol-Amine-and Carboxylic-Acid-Terminated Molecules. *J. Am. Chem. Soc.* **2006**, *128* (49), 15874–15881.
- (28) Li, Y.; Baghernejad, M.; Qusiy, A.-G.; Zsolt Manrique, D.; Zhang, G.; Hamill, J.; Fu, Y.; Broekmann, P.; Hong, W.; Wandlowski, T.; Zhang, D.; Lambert, C. Three-State Single-Molecule Naphthalene-diimide Switch: Integration of a Pendant Redox Unit for Conductance Tuning. *Angew. Chem., Int. Ed.* **2015**, *54* (46), 13586–13589.
- (29) Li, Z.; Li, H.; Chen, S.; Froehlich, T.; Yi, C.; Schönenberger, C.; Calame, M.; Decurtins, S.; Liu, S.-X.; Borguet, E. Regulating a Benzodifuran Single Molecule Redox Switch via Electrochemical Gating and Optimization of Molecule/Electrode Coupling. *J. Am. Chem. Soc.* **2014**, *136* (25), 8867–8870.
- (30) Xu, B.; Tao, N. J. Measurement of single-molecule resistance by repeated formation of molecular junctions. *Science* **2003**, *301* (5637), 1221–1223.
- (31) Venkataraman, L.; Klare, J. E.; Tam, I. W.; Nuckolls, C.; Hybertsen, M. S.; Steigerwald, M. L. Single-molecule circuits with well-defined molecular conductance. *Nano Lett.* **2006**, *6* (3), 458–462.
- (32) Guo, W.; Quainoo, T.; Liu, Z.-F.; Li, H. Robust binding between secondary amines and Au electrodes. *Chem. Commun.* **2024**, *60* (25), 3393–3396.
- (33) Kim, L.; Czyszczon-Burton, T. M.; Nguyen, K. M.; Stukey, S.; Lazar, S.; Prana, J.; Miao, Z.; Park, S.; Chen, S. F.; Inkpen, M. S. Low Vapor Pressure Solvents for Single-Molecule Junction Measurements. *Nano Lett.* **2024**, *24* (32), 9998–10005.
- (34) Kamenetska, M.; Koentopp, M.; Whalley, A.; Park, Y.; Steigerwald, M.; Nuckolls, C.; Hybertsen, M.; Venkataraman, L. Formation and evolution of single-molecule junctions. *Phys. Rev. Lett.* **2009**, *102* (12), 126803.
- (35) Reuter, M. G.; Solomon, G. C.; Hansen, T.; Seideman, T.; Ratner, M. A. Understanding and Controlling Crosstalk between Parallel Molecular Wires. *J. Phys. Chem. Lett.* **2011**, *2* (14), 1667–1671.
- (36) Kotiuga, M.; Darancet, P.; Arroyo, C. R.; Venkataraman, L.; Neaton, J. B. Adsorption-Induced Solvent-Based Electrostatic Gating of Charge Transport through Molecular Junctions. *Nano Lett.* **2015**, *15* (7), 4498–4503.
- (37) Su, T. A.; Li, H.; Steigerwald, M. L.; Venkataraman, L.; Nuckolls, C. Stereoelectronic switching in single-molecule junctions. *Nat. Chem.* **2015**, *7* (3), 215–220.
- (38) Capozzi, B.; Low, J. Z.; Xia, J.; Liu, Z.-F.; Neaton, J. B.; Campos, L. M.; Venkataraman, L. Mapping the Transmission Functions of Single-Molecule Junctions. *Nano Lett.* **2016**, *16* (6), 3949–3954.
- (39) Price, G. A.; Brisdon, A. K.; Flower, K. R.; Pritchard, R. G.; Quayle, P. Solvent effects in gold-catalysed A3-coupling reactions. *Tetrahedron Lett.* **2014**, *55* (1), 151–154.
- (40) Sherwood, J.; Clark, J. H.; Fairlamb, I. J.; Slattery, J. M. Solvent effects in palladium catalysed cross-coupling reactions. *Green Chem.* **2019**, *21* (9), 2164–2213.
- (41) Brand, J. P.; Charpentier, J.; Waser, J. Direct alkynylation of indole and pyrrole heterocycles. *Angew. Chem., Int. Ed.* **2009**, *48* (49), 9346–9349.
- (42) Stenutz, R. A collection of tables for chemistry. <https://www.stenutz.eu/> (accessed March 06, 2024). (Note: A dielectric constant for TD is determined based on the data of dodecane, ppendadecane and hexadecane).
- (43) Batra, A.; Kladnik, G.; Gorjizadeh, N.; Meisner, J.; Steigerwald, M.; Nuckolls, C.; Quek, S. Y.; Cvetko, D.; Morgante, A.; Venkataraman, L. Trimethyltin-mediated covalent gold–carbon bond formation. *J. Am. Chem. Soc.* **2014**, *136* (36), 12556–12559.